Hindawi
Advances in Civil Engineering
Volume 2021, Article ID 7526616, 10 pages
https://doi.org/10.1155/2021/7526616

Research Article

Workability and Compressive Strength Behavior of a Cemented High-Porosity Backfill Material

W. H. Cao,[1,2] **X. F. Wang**,[1,3,4] **D. S. Zhang**,[1] **X. J. Ji**,[2] **X. Z. Chen**,[2] **A. Zhang**,[2] **and F. X. Zhu**[2]

[1]*State Key Laboratory of Coal Resources and Safe Mining, China University of Mining & Technology, Xuzhou, China*
[2]*School of Civil Engineering, Nanyang Institute of Technology, Nanyang, China*
[3]*Laboratory of Mine Earthquake Monitoring and Prevention, China University of Mining & Technology, Xuzhou, China*
[4]*School of Mines, China University of Mining & Technology, Xuzhou, China*

Correspondence should be addressed to X. F. Wang; wangxufeng@cumt.edu.cn

Received 5 May 2021; Accepted 25 August 2021; Published 20 September 2021

Academic Editor: Tingting Zhang

A full understanding of the workability and unconfined compressive strength (UCS) of the cemented high-porosity (CHPB) material, made of surface sand, widely distributed in the western mining area, foam, and cementing materials, is important for applying in ecologically fragile mining areas of western China. In this article, the influence of solid content, density grade, sand/binder ratio, and silica fume dosage in binder on workability and strength development of CHPB samples in different curing ages is studied. Test results show that the fresh CHPB mix has good workability, due to the existence of a large number of bubbles. With the increase of density grade, the UCS of the CHPB sample increases exponentially. Workability of fresh CHPB samples significantly decreases with increasing solid content due to the reduction of interparticle distance. For a given mix proportion, the optimal solid content of CHPB samples is 83.7%. The variation of the sand/binder ratio from 3 to 4.5 results in a slight increase of workability and a significant increase of the UCS. Silica fume demonstrates improvement on workability and strength behavior, and the optimal dosage in the binder should not exceed 10%.

1. Introduction

Underground mining leads to a series of mining damage and environmental problems, such as the destruction of aquifer resources, surface subsidence damage to ground buildings, and surface vegetation death caused by ecological environmental damage [1, 2], which will become more prominent, with the development of coal resources gradually shifting its focus to arid and semiarid areas in western China [3]. As the most effective method to control surface subsidence and realize green mining, the filling and mining technology plays an essential role in the process of coal resource mining for its unique mining technique [4].

Filling material is the decisive factor and the bottleneck of the development of the filling mining. Over the past few decades, scholars have been looking for filling materials with sufficient raw materials, low cost, stable mechanical properties, and good fluidity. Due to the large amount of solid wastes such as waste rock, coal gangue, and tailings, the reasonable use of solid wastes to prepare composite cemented filling materials not only reduces the environmental pollution and surface waste treatment costs but also effectively reduces the cost of filling mining [5–8].

At present, with the development of cemented filling technology, remarkable achievements have been made in the preparation and properties of different solid waste cement filling materials. The particle size of gangue has a significant effect on the strength of CRF, which is also known as consolidated rockfill [9]. Cemented paste backfill (CPB) and cemented tailings backfill (CTB) are widely used in underground metal mining [10]; fly ash, blast furnace slag (slag), silica fume, pozzolanic ash, and alkali-activated materials were used as binder instead of ordinary Portland cement to reduce the cost of CPB mix [11–14]. At the same time, the properties and ratio of different types of new cementing materials, such as soil paste filling material [15],

gangue-waste concrete cemented paste backfill [16], and coal gangue backfill [17], are studied. These studies have greatly enriched the content of cemented filling materials in underground mine.

However, the main raw materials of cement paste materials, such as coal gangue, tailings, and other solid wastes, are still far less than the mining space, so it is difficult to meet the needs of filling in large-volume goaf, especially in the urgent need of green mining in mining areas of western China.

It is exciting that the western mining area is rich in surface sand. The author uses the surface sand of the mining area as the main raw material, mixes it with cementitious material into slurry, and adds foam to form the cemented high-porosity backfill (CHPB) material, which has the advantages of light weight and low cost [18]. The fresh (workability index) and hardened (unconfined compressive strength-UCS) are two main factors when designing an effective, lucrative, and sustainable CHPB matrix for underground structures [19, 20]. The main applications of CHPB in the underground mining industry are roof-contacted filling [21], small pit goaf filling [22], fire prevention, and plugging air leakage in goaf [23]. The effects of the raw material ratio and foam expansion rate on curing time and compressive strength of CHPB were studied [24], and the UCS prediction model for foam-cemented paste backfill was proposed. These studies have important reference to the research of this paper.

The objectives of this study are to therefore experimentally investigate the impacts of a number of parameters such as solid content, density grade, sand/binder ratio, and silica fume dosage on workability and strength properties of the CHPB matrix.

2. Experimental Program

2.1. Materials

2.1.1. Binder. Ordinary Portland cement (OPC) is the most common binder agent used in backfill operations due to its versatility. However, the optimization of filling material performance and the reduction of backfill cost lead to the extensive use of some pozzolanic materials, such as fly ash (FA) and blast furnace slag (slag) [19, 20].

OPC was used as binder and blended with silica fume at different replacement ratios in this study. The principal binder used is OPC (Type P.O 42.5 R, from Xuzhou, Jiangsu Province, China, based on Chinese standard GB175-2007 common Portland cement). Silica fume (from Chengdu City, Sichuan Province, China) is mainly composed of silica with a particle size of about 0.15 μm; hence, silica fume is often used as an active mineral admixture. The chemical composition of OPC and silica fume is presented in Table 1, which was measured by the X-ray fluorescence spectrometer (XRF).

2.1.2. Surface Sand. Sand used in the study was taken from the surface of Menkeqing coal mine, Ordos City, Shendong mining area, Inner Mongolia Region of China, where is rich in surface sand. Particle size distribution of the sample was determined using a laser particle size analyzer, as shown in Figure 1. The sampled surface sand has a relatively poor particle size distribution with a uniformity coefficient (Cu) of 2.5 and with particles over 0.1 mm accounted for 82.15% (over 75%), which belongs to fine sand. Meanwhile, the sample had an initial water content of around 5% and bulk density of 1.704 g/cm^3. Moreover, the crystalline components in tailings were identified using X-ray diffraction (XRD). XRD patterns displayed in Figure 2 show that the crystalline phases are predominantly quartz, albite, and potassium feldspar, which are all inert substances.

2.1.3. Foaming Agent and Water. HTQ-1 compound foaming agent developed by Huatai Building Materials Company, Henan province, China, was used in this study, of which the main raw materials are nonpolluting animal protein oil and vegetable oil and will not produce any side effects to producers, users, and the environment. Meanwhile, the foaming agent can be used under the low temperature environment. The foaming agent adopts the physical method for foaming (Figure 3(a)), which has high foaming multiple and good stability. At the same time, the bubbles are independent of each other and evenly distributed in the cement slurry, which can form a large number of closed pores (Figure 3(b)).

Tap water was used to mix the binders and fine aggregate and used for foaming solution, with a pH of 6.8.

2.2. Sample Preparation and Mix Proportion. CHPB samples with different solid contents, surface sand/binder (S/B) ratios, density grade, and silica fume in binder were prepared. First, prepare the raw materials according to the experimental project. Second, the mixture slurry was prepared by using a blender, and after diluting the foaming agent 30 times, stable foam was formed through the foaming mechanism. Then, the foam was added to the mixture slurry and stirred well to produce the desired CHPB mixture (Figure 4). The produced backfill mixtures were cast into $100 \times 100 \times 100$ mm cubic molds. Demoulded after 24 hours, the manufactured cubes were cured in the environmental chambers (Figure 5) at specific curing temperatures for periods of 7, 28, and 90 days. The relative humidity and the temperature were kept constant at $\%95 \pm 1$ and $20^{\circ}C \pm 2$, respectively. The detailed testing protocols of the CHPB mixtures are summarized in Table 2.

It should be noted that the weight of samples of the same density grade should not exceed ±50 g from the design value due to the different degree of damage of the foam in the stirring process.

2.3. Experimental Testing

2.3.1. Workability Tests. The workability of the fresh CHPB mix was evaluated by measuring the spread flow using a slump cone with the following dimensions: top diameter, 100 mm; bottom diameter, 200 mm; height, 300 mm. The

Table 1: Chemical composition of OPC and silica fume (wt. (%)).

Composition	Al_2O_3	CaO	SiO_2	Fe_2O_3	MgO	SO_3	K_2O	Na_2O	P_2O_5
OPC	4.88	64.38	19.29	3.68	2.98	3.44	1.15	0.06	0.04
Silica fume	3.5	0.6	91.5	0.9	0.3	0.5	-	0.6	-

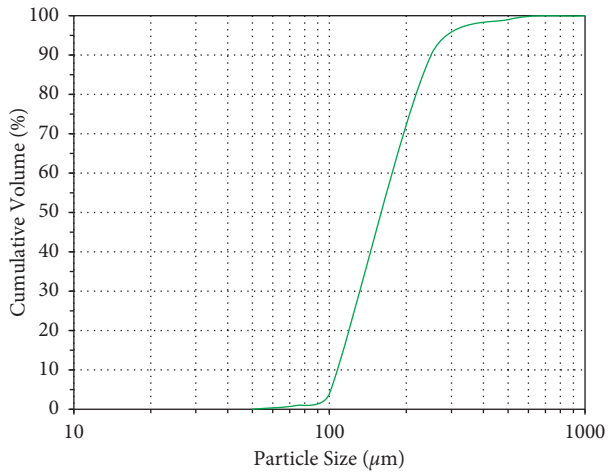

Figure 1: Particle-size distribution curves of surface sand.

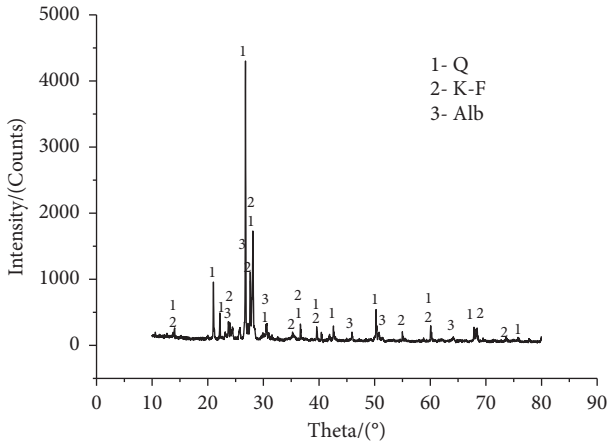

Figure 2: XRD pattern of surface sand.

final spread is measured on two perpendicular diameters 2 minutes after cone lifting. Lab tests were carried out in accordance with the Chinese standard test method for performance of ordinary concrete mixtures GB50080-2016. The estimated spread value was then calculated as the average of the two measurements (Figure 6).

At the same time, the bleeding rate of the fresh CHPB mix with different density grades was tested to reflect the water retention performance of the slurry. Under laboratory conditions, a measuring cylinder (mass m_0) was used to test the bleeding rate of slurry. The evenly stirred slurry was first added into the measuring cup to test the total weight M of the measuring cup and slurry. After standing for 3 hours, the water (mass m_1) on its surface was sucked by pipette, and the bleeding rate W was calculated:

$$W = \frac{m_1}{(M - m_0)(1 - C_m)}, \quad (1)$$

where C_m is the solid content.

2.3.2. Unconfined Compressive Strength Tests. At the predetermined curing periods (7, 28, and 90 days), unconfined compressive tests were performed on the cubic samples with a computer-controlled loading machine (Figure 7). The UCS tests were carried out at a constant deformation rate of 0.5 mm/min. Before conducting the UCS tests, the end surfaces of samples were polished to make sure that they are flat and parallel. All the measurements were carried out in triplicate, and the average values were presented in the results. The individual strengths of three specimens, molded with the same characteristics, should not deviate by more than 15% from the mean compressive strength; otherwise, an additional set of specimens needs to be prepared and tested again.

2.3.3. Microstructural Tests. Additional tests, including thermal analyses and specimen microstructure measurement, were carried out to better assess and interpret the results of the UCS tests. The phase compositions of the binder hydration products were determined by using thermal analyses (thermogravimetry (TG) and differential thermogravimetry (DTG)). TG/DTG analyses were performed on specimens at 7 d, 28 d, and 90 d for quantitative analysis of hydration products in different curing time with a PerkinElmer TGA-8000 (Figure 8) in a dynamic N_2 atmosphere at a heating rate of 10 C/min. SEM studies were done with a Quanta TM 250 operated at an accelerating voltage of 15 kV on some CHPB samples. After being soaked in anhydrous ethanol to terminate the hydration process, the specimens were taken out, dried for gold spray treatment, and put into SEM for microstructure analysis.

3. Result and Discussions

3.1. Effect of Density Grade. The overall morphology and the microstructure of specific hydration products of the CHPB specimen at 83.7% solid content cured for 28 days were scanned by the scanning electron microscope. The internal structure of the specimen is similar to honeycomb, which is mainly composed of closed pores with uniform distribution and irregular shape (Figure 9(a)). The dense structure formed by the binder wrapping surface sand is the part outside the pores (Figure 9(b)). The bonding interface of surface sand is filled with hydration products, which mainly consisted of flocculent calcium silicate gel, a certain amount of fine needle-like ettringite, and hexagonal flake calcium hydroxide crystals (Figure 9(c)).

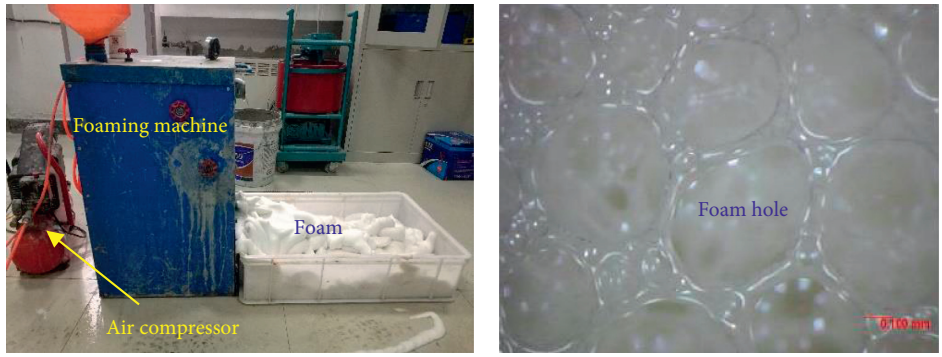

(a) (b)

Figure 3: Foams were prepared by the physical method (a) and foam microstructure (b).

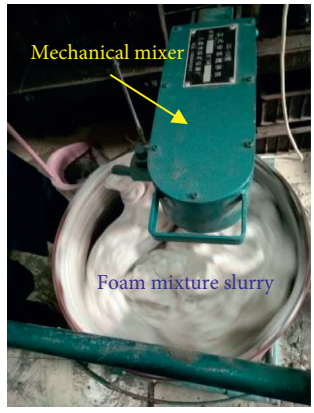

Figure 4: Mixing slurry.

Figure 5: Curing CHPB samples.

The Group D of fresh CHPB samples were prepared to investigate the influence of density grade on workability and strength development. The effect of density grade ranging from 600 kg/m^3 to 1600 kg/m^3 for CHPB mixtures (solid content of 83.7%, surface sand/binder of 3.5, and silica fume in binder of 10%) is illustrated in Figure 10. It is clear that density grade has a significant effect on the workability and strength of the sample when other ratios are constant.

As shown in Figure 10(a), when increasing density grade from 600 kg/m^3 to 1600 kg/m^3, the corresponding spread decreases by 11.5%, 9.2%, 8.2%, 5.5%, and 4.3% and the decreasing range of spread gradually slows down. At the same time, the bleeding rate of the fresh mix was 4.5%, 5.1%, 4.8%, 5.2%, 4.1%, and 3.9%, respectively. It indicates that the density grade has little effect on the bleeding rate and the mix slurry with solid content of 83.7% and surface sand/binder of 3.5, and silica fume in binder of 10% has good cohesion.

The sample strength curve with different curing times (i.e., 7 days, 28 days, and 90 days) are approximately an exponential function shown in Figure 10(b). The UCS of CHPB with 28 days curing time from 600 kg/m^3 to 1600 kg/m^3 were 0.62 MPa, 1.00 MPa, 1.57 MPa, 3.23 MPa, 8.63 MPa, and 12.00 MPa, respectively. The results shown in Figure 10(b) underline that the curing time has a significant positive role in UCS and its development of CHPB samples. For example, the UCS of CHPB samples with density grade of 1200 kg/m^3 increased from 1.95 MPa and 3.25 MPa to 3.88 MPa with increasing curing time from 7, 28, to 90 days. This increase in hydration products with curing time in the result of the TG/DTG analysis performed on 7, 28, and 90 days CHPB samples is shown in Figure 11. The DTG curves show a mass loss at 90–120°C, 440–460°C, and 720–730°C, which denote the evaporation of water along with dehydration of calcium silicate hydrate (C-S-H) and ettringite, dehydroxylation of portlandite (calcium hydroxide (C-H)), and decomposition of calcium carbonate, respectively [25]. A comparison of the DTG curves of the 7, 28, and 90 days CHPB samples shows that the peak or weight loss at around 440–460°C is higher for the latter sample. This indicates that the amount of hydration products increases with curing time since the amount of portlandite is an indication of the degree of hydration.

3.2. Effect of Solid Content. The group A of CHPB samples was prepared with different solid contents (i.e., 82.1%, 83.7%, 85.3%, and 87.0%) at density grade of 1000 kg/m^3, surface sand/binder of 3.5, and silica fume in binder of 10%. The effect of solid content on workability and strength development of CHPB samples is illustrated by Figure 12. As

Table 2: Summary of the mixture composition of the samples.

Group	Sample	Solid content (wt. (%))	Solid content proportions		Density class (kg·m^{-3})	Silica fume in binder (wt. (%))
			Binder (%)	Surface sand (%)		
A	1	82.1	22.2	77.8	1000	10
	2	83.7	22.2	77.8	1000	10
	3	85.3	22.2	77.8	1000	10
	4	87.0	22.2	77.8	1000	10
B	5	83.7	25	75	1000	10
	6	83.7	22.2	77.8	1000	10
	7	83.7	20	80	1000	10
	8	83.7	18.2	81.8	1000	10
C	9	83.7	22.2	77.8	1000	0
	10	83.7	22.2	77.8	1000	5
	11	83.7	22.2	77.8	1000	10
	12	83.7	22.2	77.8	1000	15
D	13	83.7	22.2	77.8	600	10
	14	83.7	22.2	77.8	800	10
	15	83.7	22.2	77.8	1000	10
	16	83.7	22.2	77.8	1200	10
	17	83.7	22.2	77.8	1400	10
	18	83.7	22.2	77.8	1600	10

Figure 6: Spread flow test.

Figure 7: Loading machine.

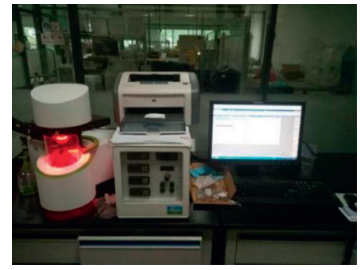

Figure 8: Thermogravimetric analyzer.

expected, the workability of fresh CHPB samples obviously decreases as the solid content rises (Figure 12(a)).

This decrease in workability with a higher solid content (lower water content) is due to the reduction in interparticle distance, thus making it easier for the solid particles to slide past one another during shearing [26, 27].

The results presented in Figure 12(b) indicate that all of the samples show a similar tendency in the time-dependent changes of the UCS. It can be noticed that when the solid content is less than 83.7%, the strength gain of CHPB samples increases with increasing solid content. This can be attributed to the content of calcium silicate hydrate (C-S-H) gel and total porosity within CHPB increasing and decreasing, respectively, with higher solid content and then resulting in denser structure and higher strength [28]. When the solid content is higher than 83.7%, the strength of CHPB samples shows a trend of negative growth with solid content increasing. This can be due to the excessively high solid content which means that the water-cement ratio is too low, resulting in insufficient hydration reaction and reducing in hydration products.

In addition, Figure 12(b) also illustrates that the UCS of CHPB increases with the elapsing of curing age regardless of solid content.

3.3. Effect of Sand/Binder Ratios. The effects of sand/binder ratios on the workability and strength of the CHPB specimens as a function of curing time are summarized in Figure 13 In this test, four different sand/binder ratios (3.0, 3.5, 4.0, and 4.5) were prepared, while other parameters such as the density grade, solid content, and silica fume in binder were maintained constant at 1000 kg/m^3, 83.7%, and 10%, respectively. It can be observed from Figure 13(a) that the spread of fresh CHPB increases slightly with an increase in the S/B ratio. That is because with the increase of the S/B ratio, the amount of sand gradually increases and the content of cementing material decreases. Due to the constant water

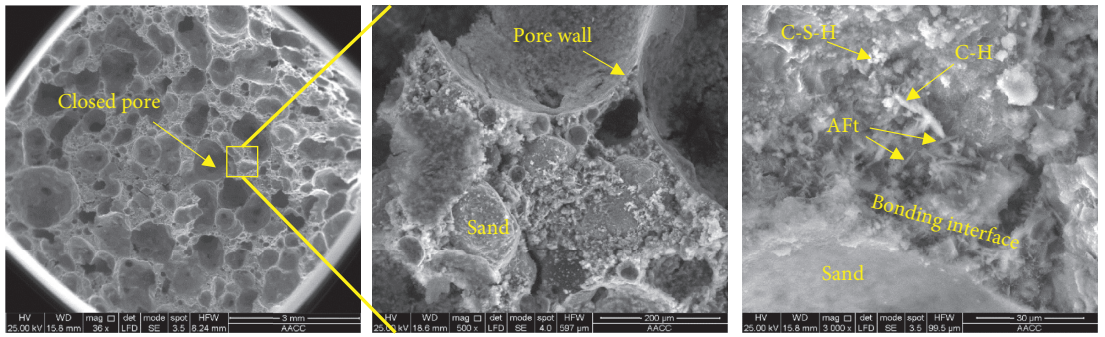

Figure 9: SEM diagram of the specimen at 83.7% solid content 28 days. (a) ×36; (b) ×500; (c) ×3000.

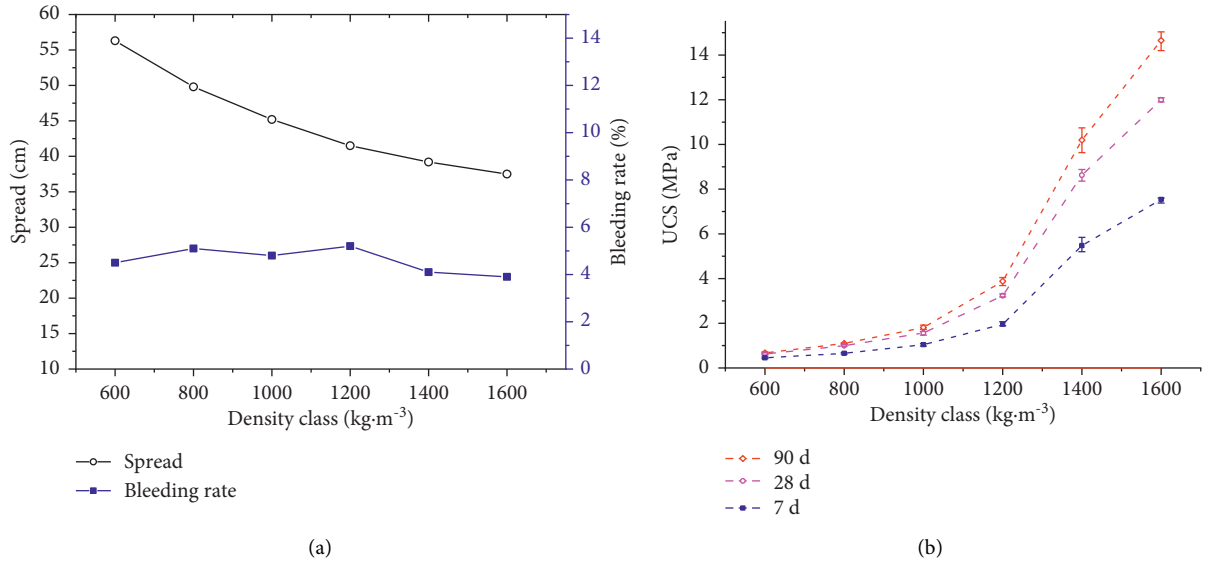

Figure 10: Effect of density grade on the (a) flow and strength of CHPB samples.

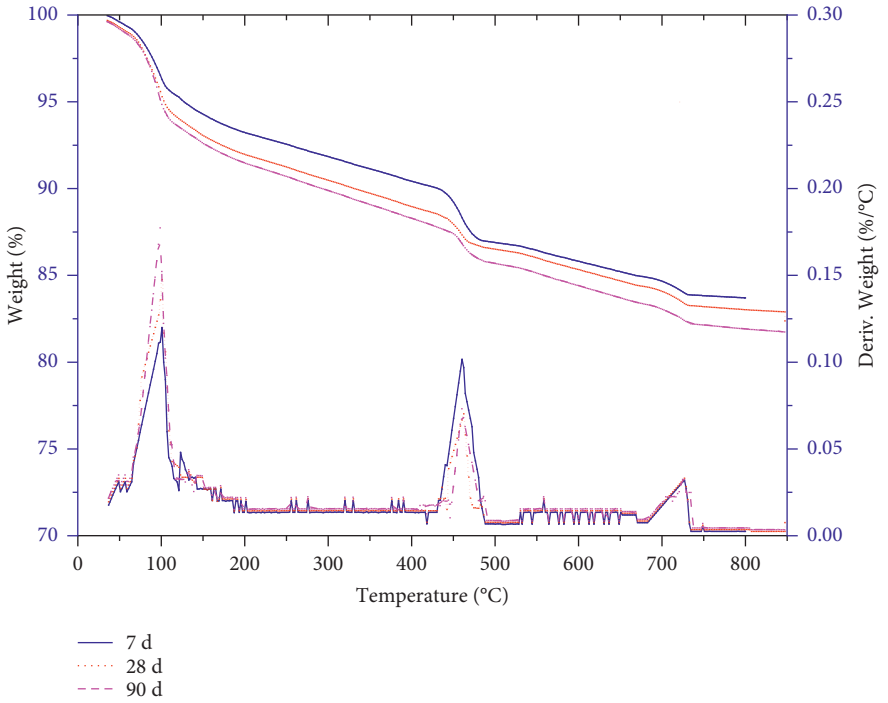

Figure 11: TG/DTG diagrams for the CHPB specimen at the density grade of 1200 kg/m^3 cured for 7, 28, and 90 days.

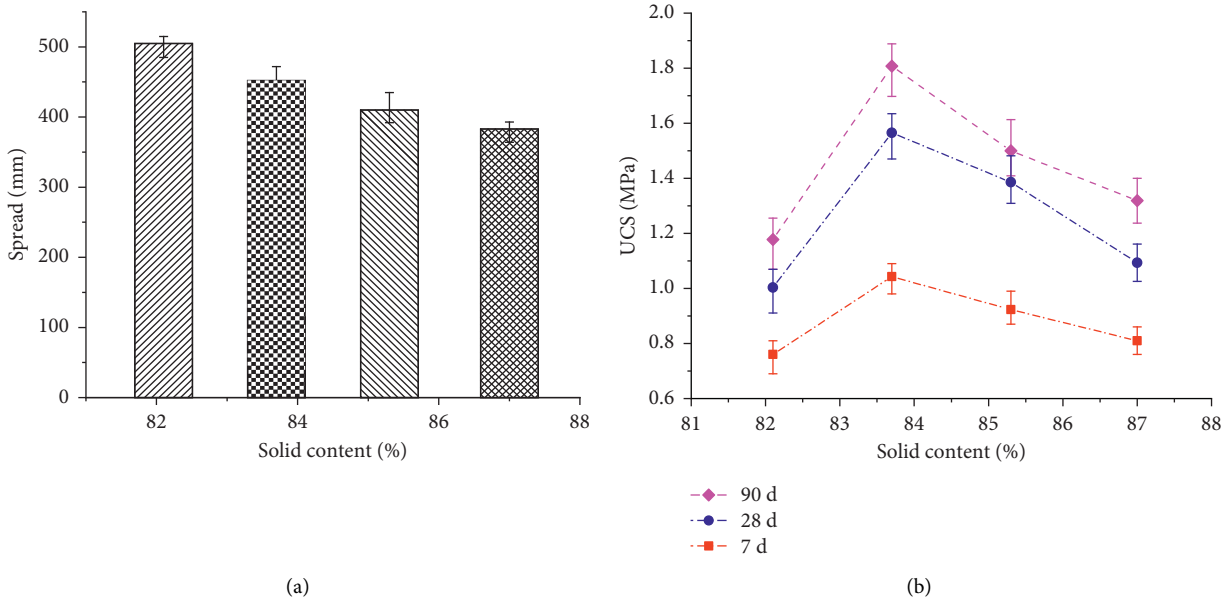

Figure 12: (a) Workability and (b) strength of CHPB samples with different solid content.

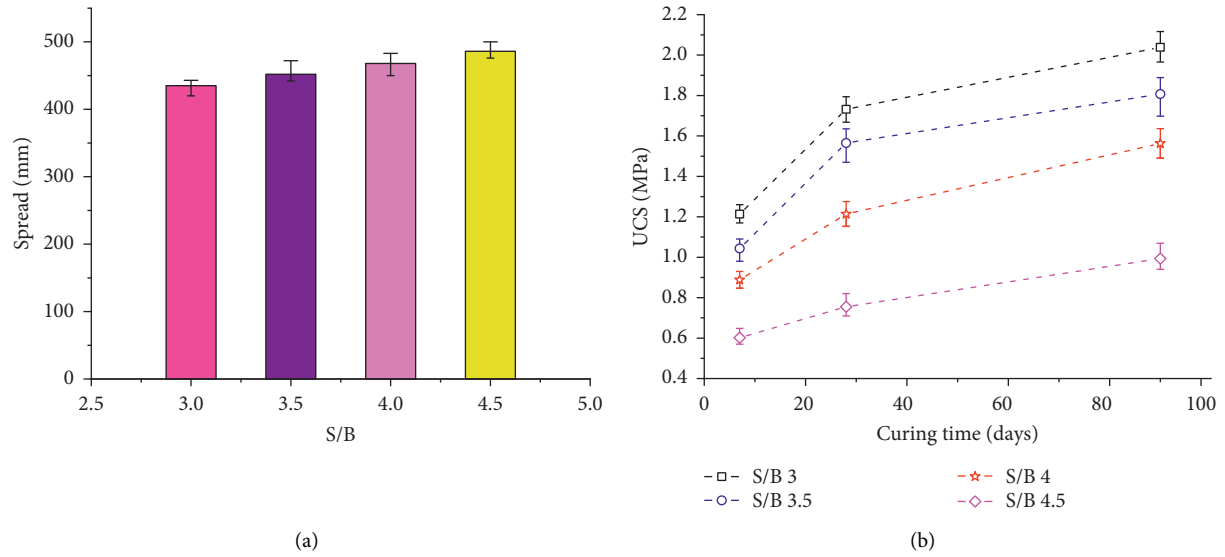

Figure 13: Influence of sand/binder ratios on the (a) workability and (b) strength of CHPB samples.

content, on the one hand, the corresponding water-binder ratio increases, and on the other hand, the encapsulation of cementing materials to sand decreases.

From Figure 13(b), it is obvious that the variation of the S/B ratio from 3 to 4.5 results in a decrease of the strength of CHPB. It is mainly due to the reduction of the relative content of cementing materials, resulting in the reduction of hydration products and the encapsulation force of mortar. At the same time, the increase of the water-binder ratio also reduces the compactness of structure. The results presented in Figure 13(b) indicate that all of the samples have a rapid increase in the UCS until 28 days and then a steady increase. This is due to the fact that cementitious materials develop strength with continual hydration. The rate of strength gain is faster at the early ages but reduced with curing time [29].

3.4. Effect of Silica Fume in Binder. Figure 14 demonstrates the strength development of CHPB samples produced by using a silica fume in binder of 0–15 wt%. The laboratory tests were conducted at a fixed solid content of 83.7%, a sand/binder ratio of 3.5, and a density grade of 1000 kg/m^3. From Figure 14(a), it is fairly obvious that the spread of fresh CHPB is slightly improved with an increase in silica fume

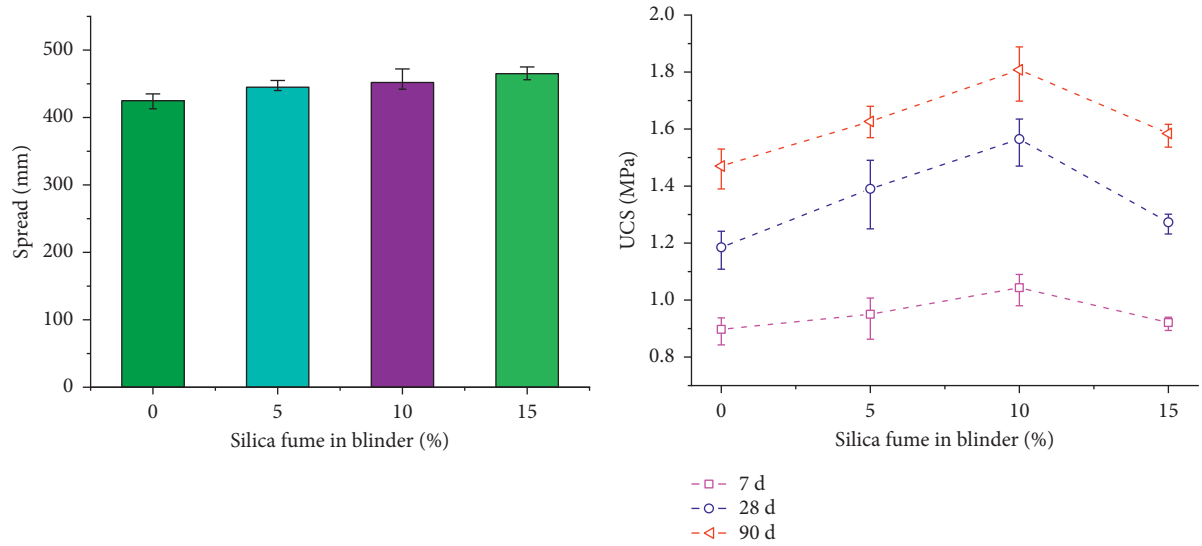

(a) (b)

Figure 14: (a) Workability and (b) strength of CHPB samples with various silica fume in binder.

dosage in binder. An explanation for this behavior is that higher replacement of processing silica fume results in a reduction of friction between particles [30].

The results presented in Figure 14(b) underline that silica fume dosage in binder has a significant impact on the strength of CHPB. The UCS increases with the dosage up to 10% and then starts to decrease with higher dosage. The optimum dosage that produces the highest compressive strength of the CHPB appears to be about 10%. This can be explained by the following: (i) silica can react with calcium hydroxide (C-H) to form calcium silicate gel. At low dosage, an increase in silica fume leads to more amount of hydration products. (ii) The particle size of silica fume is smaller than that of cement, which can increase the compactness of the internal structure.

Subsequently, this strength is observed to deteriorate gradually as the dosage increase from 10% to 15%.

The reasons for the contrasting trend could be due to excessive silica powder which will reduce the amount of water involved in the hydration reaction, resulting in a decrease in the amount of early hydration products, unable to generate sufficient amount of C-H. At the same time, the agglomeration phenomenon occurs, which reduces the compactness of the material and causes its strength to decrease.

4. Conclusions

In this paper, a comprehensive laboratory test work has been conducted to study the influences of four parameters (i.e., solid content, sand/binder ratios, density grade, and silica fume dosage in binder) on workability and strength development of CHPB samples. For given CHPB samples with different density grades (i.e., 600 kg/m^3, 800 kg/m^3, 1000 kg/m^3, 1200 kg/m^3, 1400 kg/m^3, and 1600 kg/m^3), sand/binder ratio (i.e., 3, 3.5, 4, and 4.5), solid content (i.e., 82.1%, 83.7%, 85.3%, and 87.0%), and silica fume dosage in binder (i.e., 0%, 5%, 10%, and 15%) were prepared to obtain the workability and UCS at different curing times (i.e., 7 d, 28 d, and 90 d). Based on the results of the experimental tests performed, the following conclusions can be drawn:

(1) The internal structure of the CHPB sample contains a large number of closed pores. With the increase of the density grade, the number of pores decreases, and the UCS of the sample increases exponentially. On the contrary, the workability of the samples decreases significantly.

(2) Workability of fresh CHPB samples significantly decreases with increasing solid content due to the reduction of interparticle distance. The UCS increases with increasing solid content from 82.1% to 83.7% through a denser structure. However, a decrease trend in UCS is observed as the solid content exceeds 83.7%.

(3) The variation of the sand/binder ratio from 3 to 4.5 results in a slight increase of workability and a significant increase of the strength. It is mainly due to the reduction of the relative content of cementing materials, resulting in the reduction of hydration products. At the same time, the increase of the water-binder ratio also reduces the compactness of the structure.

(4) Adding silica fume poses a positive effect of silica fume dosage on workability behavior and UCS of CHPB samples. The optimum dosage in binder that produces the highest compressive strength of the CHPB appears to be about 10%.

Data Availability

The data used to support the findings of this study are available from the corresponding author upon request.

Conflicts of Interest

The authors declare that they have no conflicts of interest.

Acknowledgments

The work was supported by Independent Research Project of State Key Laboratory of Coal Resources and Safe Mining, CUMT (SKLCRSM19X005), National Key Research and Development Program of China (2018YFC0604705), Henan Province Key Scientific Research Projects of Colleges and Universities (20A440010) and Interdisciplinary Sciences Project, Nanyang Institute of Technology, Key R&D and Promotion Projects in Henan Province (212102310030), and Doctoral Research Start-Up Fund Project of Nanyang Institute of Technology.

References

[1] M. Fall, J. C. Célestin, M. Pokharel, and M. Touré, "A contribution to understanding the effects of curing temperature on the mechanical properties of mine cemented tailings backfill," *Engineering Geology*, vol. 114, no. 3, pp. 397–413, 2010.

[2] W. Yu, B. Pan, F. Zhang, S. Yao, and F. Liu, "Deformation characteristics and determination of optimum supporting time of alteration rock mass in deep mine," *KSCE Journal of Civil Engineering*, vol. 23, no. 11, pp. 4921–4932, 2019.

[3] D. S. Zhang, W. P. Li, X. P. Lai, G. W. Fan, and W. Q. Liu, "Development on basic theory of water protection during coal mining in northwest of China," *China Coal Society*, vol. 42, no. 1, pp. 36–43, 2017.

[4] M. G. Qian and X. X. Miao, "Research on green mining of coal resources in China: current S tatus and future prospects," *Journal of Mining & Safety Engineering*, vol. 26, no. 1, pp. 1–14, 2009.

[5] A. A. Hammond, "Mining and quarrying wastes: a critical review," *Engineering Geology*, vol. 25, no. 1, pp. 17–31, 1988.

[6] Q. Chen, Y. Tao, Y. Feng, Q. Zhang, and Y. Liu, "Utilization of modified copper slag activated by Na2SO4 and CaO for unclassified lead/zinc mine tailings based cemented paste backfill," *Journal of Environmental Management*, vol. 290, Article ID 112608, 2021.

[7] H. Jiang, M. Fall, and L. Cui, "Freezing behaviour of cemented paste backfill material in column experiments," *Construction and Building Materials*, vol. 147, pp. 837–846, 2017.

[8] W. Sun, K. Hou, Z. Yang, and Y. Wen, "X-ray CT three-dimensional reconstruction and discrete element analysis of the cement paste backfill pore structure under uniaxial compression," *Construction and Building Materials*, vol. 138, pp. 69–78, 2017.

[9] H. Jiang, M. Fall, Y. li, and J. Han, "An experimental study on compressive behaviour of cemented rockfill," *Construction and Building Materials*, vol. 213, pp. 10–19, 2019.

[10] J. S. Chen, B. Zhao, X. M. Wang, Q. L. Zhang, and L. Wang, "Cemented backfilling performance of yellow phosphorus slag," *International Journal of Minerals, Metallurgy, and Materials*, vol. 17, no. 1, pp. 121–126, 2010.

[11] Y. Wang, M. Fall, and A. Wu, "Initial temperature-dependence of strength development and self-desiccation in cemented paste backfill that contains sodium silicate," *Cement and Concrete Composites*, vol. 67, pp. 101–110, 2016.

[12] Q. L. Zhang, Y. T. Li, Q. S. Chen, Y. K. Liu, Y. Feng, and D. L. Wang, "Effects of temperatures and pH values on rheological properties of cemented paste backfill," *Journal of Central South University*, vol. 28, no. 6, pp. 1707–1723, 2021.

[13] D. L. Wang, Q. L. Zhang, Q. S. Chen, C. C. Qi, Y. Feng, and C. C. Xiao, "Temperature variation characteristics in flocculation settlement of tailings and its mechanism," *International Journal of Minerals, Metallurgy and Materials*, vol. 27, no. 11, pp. 1438–1448, 2020.

[14] H. Jiang, Z. Qi, E. Yilmaz, J. Han, J. Qiu, and C. Dong, "Effectiveness of alkali-activated slag as alternative binder on workability and early age compressive strength of cemented paste backfills," *Construction and Building Materials*, vol. 218, pp. 689–700, 2019.

[15] Z. Wang, W. J. Yu, and F. F. Liu, "The materialization characteristics and ratio of a new soil paste filling material," *Advances in Civil Engineering*, vol. 2020, Article ID 6645494, 8 pages, 2020.

[16] G. R. Feng, X. Q. Jiang, Y. X. Guo, and T. Qi, "Study on mixture ratio of gangue-waste concrete cemented paste backfill," *Journal of Mining & Safety Engineering*, vol. 33, no. 6, pp. 1072–1079, 2016.

[17] D. Wu, Y. Hou, T. Deng, Y. Chen, and X. Zhao, "Thermal, hydraulic and mechanical performances of cemented coal gangue-fly ash backfill," *International Journal of Mineral Processing*, vol. 162, pp. 12–18, 2017.

[18] X. F. Wang, W. H. Cao, and D. S. Zhang, "Mechanism study on influence of particle size and content of gangue on strength of high-sand and high-foam cement-based filling material," *Journal of Mining & Safety Engineering*, vol. 37, no. 2, pp. 2376–2384, 2020.

[19] D. Ouattara, T. Belem, M. Mbonimpa, and A. Yahia, "Effect of superplasticizers on the consistency and unconfined compressive strength of cemented paste backfills," *Construction and Building Materials*, vol. 181, pp. 59–72, 2018.

[20] E. Yilmaz, T. Belem, B. Bussière, and M. Mamert, "Curing time effect on consolidation behaviour of cemented paste backfill containing different cement types and contents," *Construction and Building Materials*, vol. 75, pp. 99–111, 2015.

[21] J. P. Cui, Z. B. Guo, L. Li, S. Zhang, Y. Zhao, and Z. Ma, "A hybrid artificial intelligence model for predicting the strength of foam-cemented paste backfill," *IEEE Access*, vol. 8, Article ID 84569, 2020.

[22] W. Y. Cai, Z. C. Chang, D. S. Zhang, X. Wang, W. Cao, and Y. Zhou, "Roof filling control technology and application to mine roadway damage in small pit goaf," *International Journal of Mining Science and Technology*, vol. 29, pp. 477–482, 2019.

[23] H. Wen, D. Zhang, Z. J. Yu, X. Zheng, S. Fan, and B. Laiwang, "Experimental study and application of inorganic solidified foam filling material for coal mines," *Advances in Materials Science and Engineering*, vol. 2017, Article ID 3419801, 13 pages, 2017.

[24] Q. P. Wang, H. Wang, and F. F. Min, "Effect of raw material ratio on properties of foam paste backfilling materials," *Materials Review*, vol. 29, pp. 135–139, 2015.

[25] N. Lemonis, P. E. Tsakiridis, N. S. Katsiotis et al., "Hydration study of ternary blended cements containing ferronickel slag and natural pozzolan," *Construction and Building Materials*, vol. 81, no. 11, pp. 130–139, 2015.

[26] D. Simon and M. Grabinsky, "Apparent yield stress measurement in cemented paste backfill," *International Journal of Mining, Reclamation and Environment*, vol. 27, no. 4, pp. 231–256, 2013.

[27] H. Q. Jiang, M. Fall, and C. Liang, "Yield stress of cemented paste backfill in sub-zero environments: experimental results," *Minerals Engineering*, vol. 92, pp. 141–150, 2016.
[28] M. Fall, M. Benzaazoua, and E. G. Saa, "Mix proportioning of underground cemented tailings backfill," *Tunnelling and Underground Space Technology*, vol. 23, no. 1, pp. 80–90, 2008.
[29] A. M. Neville, *Properties of Concrete*, Prentice-Hall, London, England, 2000.
[30] A. Sathonsaowaphak, P. Chindaprasirt, and K. Pimraksa, "Workability and strength of lignite bottom ash geopolymer mortar," *Journal of Hazardous Materials*, vol. 168, no. 1, pp. 44–50, 2009.